Ball lens coupled fiber-optic probe for depth-resolved spectroscopy of epithelial tissue

Richard A. Schwarz, Dizem Arifler, Sung K. Chang, Ina Pavlova, Insiya A. Hussain, Vivian Mack, Bob Knight, and Rebecca Richards-Kortum

Department of Biomedical Engineering, University of Texas at Austin, 1 University Station, C0800, Austin, Texas 78712

Ann M. Gillenwater

Department of Head and Neck Surgery, University of Texas M. D. Anderson Cancer Center, 1515 Holcombe Boulevard, Houston, Texas 77030

Received September 8, 2004

A ball lens coupled fiber-optic probe design is described for depth-resolved measurements of the fluorescence and reflectance properties of epithelial tissue. A reflectance target, fluorescence targets, and a two-layer tissue phantom consisting of fluorescent microspheres suspended in collagen are used to characterize the performance of the probe. Localization of the signal to within 300 μm of the probe tip is observed by use of reflectance and fluorescence targets in air. Differential enhancement of the fluorescence signal from the top layer of the two-layer tissue phantom is observed. © 2005 Optical Society of America

OCIS codes: 170.6510, 170.3890, 060.2310.

Optical spectroscopy is emerging as an effective diagnostic technique for noninvasive detection of cancers and precancers that originate in the epithelial lining of organs such as the uterine cervix, the oral cavity, the urinary bladder, and the esophagus.[1] The progression of precancer in these tissues produces morphologic and biochemical changes in the epithelium and supporting stroma. These changes include alterations in epithelial cell morphology and metabolic activity, changes in stromal protein morphology and cross-linking, and increasing stromal angiogenesis. As a result, the concentration and distribution of endogenous fluorophores such as reduced nicotinamide adenine dinucleotide, flavin adenine dinucleotide, keratin, tryptophan, and collagen cross-links, and absorbers such as hemoglobin, are altered with the progression of precancer.[2] Thus knowledge of the depth-dependent distribution of chromophores may have important diagnostic significance.

Endogenous chromophores can be detected noninvasively *in vivo* by use of fiber-optic fluorescence and reflectance spectroscopy. Many fiber-optic probe designs collect the integrated signal from both the epithelium (which is typically of the order of 300 μm thick) and the underlying stroma. In these systems, sophisticated analysis strategies are required for deconvolution of spectroscopic data to yield quantitative concentrations of chromophores, and little information about depth-related changes is obtained. Fiber probes that can localize spectroscopic information by depth to distinguish epithelial and stromal optical signatures should improve the ability of spectroscopy to evaluate noninvasively the progression of precancerous changes.

A variety of probe designs for obtaining localized or depth-resolved spectroscopic data have been reported.[3,4] Single-fiber probe configurations, in which the same fiber is used for illumination and collection, are sensitive to light scattering from superficial tissue regions.[5,6] However, the use of single-fiber probes for optical measurements is limited by lower signal-to-noise ratios that are due to autofluorescence generated by impurities in the fiber core and by specular reflection from fiber surfaces. With multiple-fiber probes, many configurations are possible. Straight-fiber geometries with different source–detector separations permit some depth discrimination; however, in epithelial tissue the signal from the stroma tends to dominate, even at minimum source–detector separation.[7] Angled illumination and collection fibers can be used to target specific depth regions.[8,9] Targeting the epithelial layer, however, requires steep angles that may be impractical for clinical probe designs. Other strategies include variation of the diameters of the illumination and collection fibers and variation of the probe-to-tissue distance.[10]

Spherical tips and ball lenses have been used for a variety of purposes in optical probes for biomedical applications. Spherical tips have been employed to improve light delivery in photodynamic therapy.[11] On-axis configurations that use ball lenses and half-ball lenses have been described.[4] A ball lens probe with a central illumination fiber surrounded by collection fibers was used for signal enhancement in Raman spectroscopy of tissue.[12]

In this Letter we describe the design and characterization of a ball lens coupled, multiple-fiber contact probe for depth-resolved fluorescence and reflectance spectroscopy of epithelial tissue. Different source–detector separations used in combination with a sapphire ball lens provide a variable geometric overlap between the illumination and collection regions, facilitating depth discrimination. The probe design is illustrated in Fig. 1(a). The illumination and collection fibers have a core diameter of 200 μm and a numerical aperture of 0.22. The fiber ends are separated from the sapphire ball lens by a 0.5-mm air gap. The collection fiber is positioned on the central axis of the ball lens, and two illumination fibers are symmetrically positioned off axis.

0146-9592/05/101159-3/$15.00

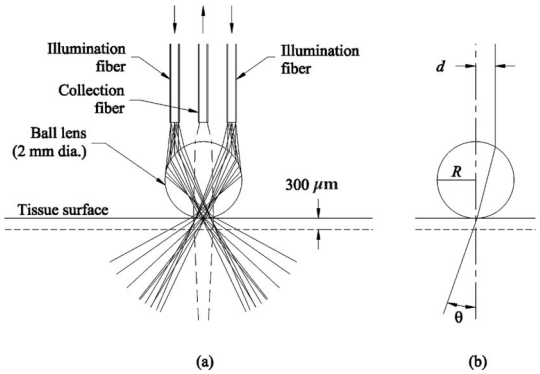

Fig. 1. (a) Ball lens coupled probe, showing illumination ray paths (solid lines) and collection region (dashed lines). A typical epithelial thickness of 300 μm is shown for reference. (b) Angular deviation of a ray incident parallel to the probe axis.

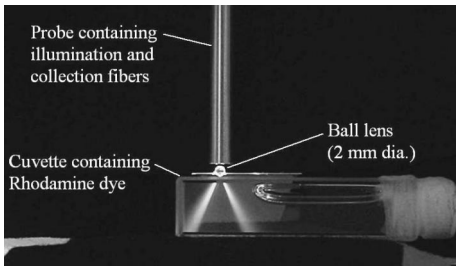

Fig. 2. Photograph of the ball lens coupled probe illuminating a cuvette containing the fluorescent dye Rhodamine.

The angle at which the illumination paths intersect the collection region grows steeper with increasing source–detector separation and with decreasing ball lens diameter. As shown in Fig. 1(b), a ray traveling in air that enters the ball lens parallel to the probe axis at a displacement d from the centerline experiences a total angular deviation θ as it passes through the lens and exits into tissue:

$$\theta = \sin^{-1}\left(\frac{d}{R}\right) - 2\sin^{-1}\left(\frac{d}{Rn_L}\right) + \sin^{-1}\left(\frac{d}{Rn_T}\right), \quad (1)$$

where d is the displacement from centerline, R and n_L are the radius and the refractive index of the ball lens, respectively, and n_T is the refractive index of the tissue. Depth localization of the detected signal is determined by the overlap of the angled illumination rays and the collection region. Wavelength alone may also have an effect on the penetration depth, a factor that is not included in this model. Maximum sensitivity to the superficial tissue region is achieved when the illumination paths intersect the detection cone at the distal surface of the ball lens and then diverge rapidly. The diverging illumination beams are visible in Fig. 2, which is a photograph of the ball lens coupled probe illuminating a quartz cuvette containing the fluorescent dye Rhodamine.

The performance of the ball lens coupled probe design was characterized experimentally with a 2-mm-diameter ball lens and center-to-center source–detector separations of 500 and 750 μm. The ball lens was supplied by Edmund Industrial Optics (Barrington, N.J.). The experimental setup included a xenon light source (ISA, Inc., Edison, N.J.); bandpass filter (Chroma Technology Corporation, Rockingham, Vt.); a ball lens coupled probe; an imaging spectrograph (Chromex 250is); and a TE-cooled CCD detector (DV420-BU, Andor Technology, South Windsor, Conn.). Experiments to evaluate depth localization were conducted with a reflectance target at a variable distance, fluorescence targets at a variable distance, and a two-layer tissue phantom in contact with the probe.

For the experiments involving targets at a variable distance, a thin reflective or fluorescent target was placed near the tip of the probe (in air) and the intensity of the detected reflectance or fluorescence signal was measured as a function of probe-to-target distance. The reflectance target was a 125-μm-thick sheet of white business paper (Southworth P403C). The fluorescence targets were single-layer tissue phantoms of 400-μm nominal thickness consisting of fluorescent polystyrene microspheres (Bangs Laboratories, Fishers, Ind.) embedded in collagen gels. The procedure used for the preparation of the collagen gels was described previously.[13] Three types of fluorescent microsphere were used, with the following excitation–emission peak wavelengths, diameters, and concentrations: (a) 370–425 nm, 1.89-μm diameter, 1.2×10^9 spheres/mL; (b) 450–490 nm, 2.72-μm diameter, 5.7×10^8 spheres/mL; (c) 633-650–680 nm, 5.49-μm diameter, 5.0×10^7 spheres/mL. The scattering parameters of each tissue phantom were calculated by Mie theory at the corresponding excitation wavelength. The contribution of collagen to the total scattering and fluorescence is not significant because of its low concentration in the gel. The calculated values roughly approximate the scattering parameters of epithelial tissue[14]: (a) $\mu_s = 79\ \mathrm{cm}^{-1}$, $g = 0.93$; (b) $\mu_s = 57\ \mathrm{cm}^{-1}$, $g = 0.90$; (c) $\mu_s = 30\ \mathrm{cm}^{-1}$, $g = 0.92$.

Results obtained with the reflectance target are displayed in Fig. 3. For the 750-μm source–detector separation the normalized intensity drops to half-maximum at an average probe-to-target distance of 136 μm and to 10% of maximum at an average distance of 274 μm. For the 500-μm source–detector separation the normalized intensity drops to half-maximum at an average distance of 340 μm and to 10% of maximum at an average distance of 565 μm. Similar results were obtained with the single-layer fluorescence targets (not shown).

The two-layer tissue phantom consisted of two stacked layers of fluorescent microspheres suspended in collagen, each 400 μm thick, and was prepared identically to single-layer phantoms (a) and (b) described above. The probe was placed in contact with the tissue phantom, and fluorescence emission spectra were obtained at 370- and 450-nm excitation sequentially. Excitation at 370 nm preferentially excites fluorescence in the top layer and some residual fluorescence in the bottom layer, whereas 450-nm excitation preferentially excites fluorophores in the bottom layer. These measurements were performed with a straight-fiber probe (no ball lens; single illumina-

tion fiber with adjacent collection fiber at 250-μm source–detector spacing), and with the ball lens coupled probe configuration selected for optimum depth localization (two illumination fibers with a 2-mm-diameter ball lens and 750-μm source–detector separation). Excitation power values in the straight-fiber configuration were 0.30 μW (370 nm) and 2.4 μW (450 nm); in the ball lens configuration, 0.45 μW (370 nm) and 3.4 μW (450 nm). The exposure time was 1 s in all cases. To facilitate comparison, all two-layer phantom fluorescence spectra were background corrected and divided by the corresponding excitation energy.

Figures 4 and 5 show the detected fluorescence signal at 370- and 450-nm excitation from the two-layer phantom. Relative to the straight-fiber probe configuration (Fig. 4), the ball lens probe configuration (Fig. 5) collects 3.8 times as much fluorescence signal from the top layer and 0.74 times as much fluorescence signal from the bottom layer. In the straight-fiber case the 370-nm excited fluorescence spectrum displays a shoulder that is due to the fact that the bottom layer does produce some fluorescence at 370-nm excitation. This contribution from the lower layer is significantly reduced by the use of the ball lens coupled probe.

These preliminary results indicate that the ball lens coupled fiber-optic probe has the potential to facilitate depth-resolved measurements of the reflectance and fluorescence properties of tissue. The depth profile of the probe is controllable through the selection of source–detector fiber spacing and ball lens diameter. The geometry described here can be extended to concentric rings of illumination fibers to increase the signal-to-noise ratio. The ability to target the epithelium selectively may improve the performance of optical spectroscopy as a diagnostic tool for detection of cancers that originate in epithelial tissue.

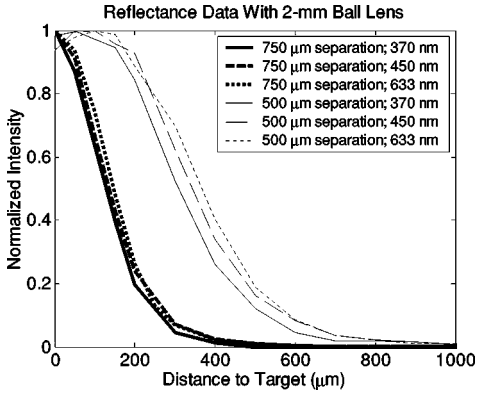

Fig. 3. Normalized reflectance signal as a function of probe-to-target distance. Source–detector separation and illumination wavelength are noted. Half-maximum intensity occurs at an average distance of 136 μm (for 750-μm separation) or 340 μm (for 500-μm separation).

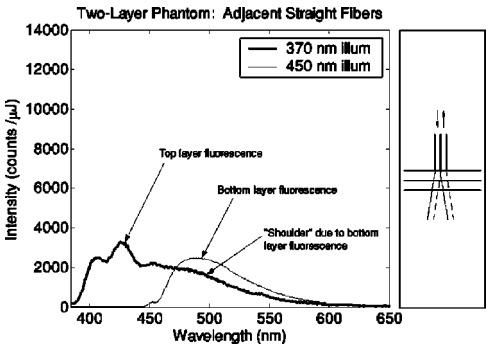

Fig. 4. Two-layer tissue phantom fluorescence data: straight fiber probe at a minimum source–detector separation (250 μm), corrected for excitation energy.

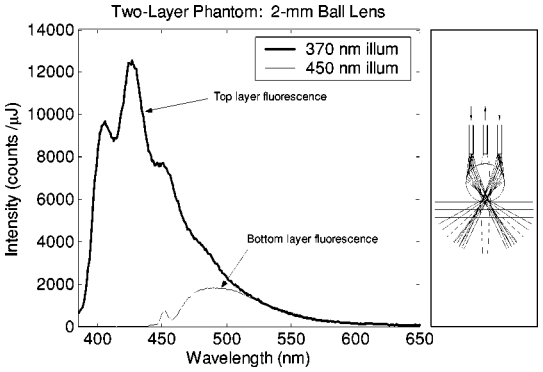

Fig. 5. Two-layer tissue phantom fluorescence data: ball lens coupled probe with a 2-mm-diameter ball lens and 750-μm source–detector separation, corrected for excitation energy.

The authors gratefully acknowledge support from National Cancer Institute grant R01 CA095604.

References

1. G. A. Wagnieres, W. M. Star, and B. C. Wilson, Photochem. Photobiol. **68**, 603 (1998).
2. R. Drezek, K. Sokolov, U. Utzinger, I. Boiko, A. Malpica, M. Follen, and R. Richards-Kortum, J. Biomed. Opt. **6**, 385 (2001).
3. T. J. Pfefer, L. S. Matchette, A. M. Ross, and M. N. Ediger, Opt. Lett. **28**, 120 (2003).
4. U. Utzinger and R. Richards-Kortum, J. Biomed. Opt. **8**, 121 (2003).
5. A. Amelink, M. P. L. Bard, S. A. Burgers, and H. J. C. M. Sterenborg, Appl. Opt. **42**, 4095 (2003).
6. B. W. Pogue and G. Burke, Appl. Opt. **37**, 7429 (1998).
7. C. Zhu, Q. Liu, and N. Ramanujam, J. Biomed. Opt. **8**, 237 (2003).
8. M. C. Skala, G. M. Palmer, C. Zhu, Q. Liu, K. M. Vrotsos, C. L. Marshek-Stone, A. Gendron-Fitzpatrick, and N. Ramanujam, Lasers Surg. Med. **34**, 25 (2004).
9. L. Nieman, A. Myakov, J. Aaron, and K. Sokolov, Appl. Opt. **43**, 1308 (2004).
10. T. J. Pfefer, K. T. Schomacker, M. N. Ediger, and N. S. Nishioka, Appl. Opt. **41**, 4712 (2002).
11. R. M. Verdaasdonk and C. Borst, in *Optical-Thermal Response of Laser-Irradiated Tissue*, A. J. Welch and M. J. C. van Gemert, eds. (Plenum, New York, 1995), p. 619.
12. J. T. Motz, M. Hunter, L. H. Galindo, J. A. Gardecki, J. R. Kramer, R. R. Dasari, and M. S. Feld, Appl. Opt. **43**, 542 (2004).
13. K. Sokolov, J. Galvan, A. Myakov, A. Lacy, R. Lotan, and R. Richards-Kortum, J. Biomed. Opt. **7**, 148 (2002).
14. T. Collier, D. Arifler, A. Malpica, M. Follen, and R. Richards-Kortum, IEEE J. Sel. Top. Quantum Electron. **9**, 307 (2003).